# Identification of nano-phases: relative merit of local analysis techniques (HRTEM, nanodiffraction, EDS/EELS)

**Philippe-André Buffat**

**Centre Interdisciplinaire de Microscopie Electronique, Ecole Polytechnique Fédérale de Lausanne**

## Abstract:

Information for phase identification may be gathered in the electron transmission microscope with spatial resolution down to the nanometre scale. Energy dispersive X-ray and electron energy loss spectrometries are based on inelastic electron-sample interaction. They have the advantage to give a direct knowledge of the chemical nature of the atoms under the electron probe, sometimes also with valence and bonding, but concentrations are mean values over all atoms in the volume excited that may be insufficient when composition is not uniform. Moreover, X-ray absorption, electron scattering and channelling may lead to errors hard to notice and correct. Elastic interaction is observed on diffraction patterns for crystalline phases with the advantage that superimposed patterns in the case of mixtures are easily distinguished in most cases. It leads to phase identification via crystallographic databases. When the scale of investigation goes down to a few nanometres or tens of nanometres, indexing diffractograms of high-resolution transmission electron microscopy images is attractive, but it is often forgotten that such diffractograms are not diffraction patterns of the crystal itself and that lattice spacings may even be shifted by several per-cents in rounded nanoparticles.

## Introduction[1]:

Progress in modelling and understanding chemico-physical properties has shown that the very intricate structure of the matter is often essential in explaining the bulk materials properties. Electron microscopy and its associated analytical techniques obviously play a key role in this effort since the middle of the last century as for instance it validates the mathematical model of dislocation proposed half a century before to explain plasticity of metals and alloys. Electron energy loss spectrometry with high spatial and energy resolution opens now new understanding of electron mobility and local band structure in nanostructured material [1]. As new technologies develop based on the assumption that the finer the structure of materials the better their properties, the so called "nanotechnologies", the need for more detailed views of the microstructure and analytical capabilities to finer scale will still grow.

Phase identification may be taken in several understandings. In its strictly physical meaning: is an object solid, liquid or gaseous is a question that receives an

1 This paper is part of a lecture presented at the 1st Stanisław Gorczyca Summer School on Advanced Transmission Electron Microscopy 30.6-5.7.2003, Kraków

immediate and obvious answer. But in which class to put an ice cream? Are nano-bubbles from implanted rare gas in alloys always gaseous?

In this talk, we consider phase identification as the knowledge of the chemical composition together with the allotropic form for each compound present in the sample. Analytical electron microscopy looks often as the easiest if not the only route to get at the same time and place morphological, crystallographic and chemical information with a spatial resolution down to the nanometre if not to the atomic scale. This leadership weakens when information is sought on sub-nanometre particles or for isotope distribution where field ion microscopy and its mass spectrometry capability (APFIM, 3DAP[1]) allow an analysis atom by atom but at the expense of a tedious sample preparation and a lengthy observation (see for instance Blavette [2] and Cerezo [3]). It should not be forgotten also that organic material constitutes a large field where phase identification by TEM remains at best difficult in a favourable cases, or even impossible (think about amorphous or imperfectly crystallized materials, isomers and polymers, high sensitivity to irradiation damage...).

## EDS and EELS spectrometries

Inelastic interaction where the incident electron dissipates part of its kinetic energy to ionise the target atom leads to direct chemical information. For technical reasons, X-ray energy dispersive spectrometry (EDS) is better suited to analyse ionisation of deep core levels energy and gives quite easily qualitative and semi-quantitative, if not quantitative, elemental analysis. At contrary, energy loss (EELS) spectroscopy is mostly performed between 0 and 2 keV on outer electron shells and is thus sensitive to atom bonding and valence effects, a much richer information at the price of a more complex spectrum interpretation and the preparation of samples thin enough to avoid an excessive convolution between low and core energy losses

Five factors of different types ultimately limit the accuracy of the analysis by spectrometries:

i) Statistical relevancy requires recording a high number of events. Figure 1 summarises the limits of phase identification by EDS in calcium phosphates analysis. These minerals are of importance in biological studies (natural bone and scaffolds, implant coatings and cements, blood vessel and cardiac valves mineralization...) and most often the phase is only assessed on the base of the calcium to phosphorus ratio. In this sample, already characterized by electron diffraction and HRTEM [4], a synthetic octcalcium phosphate (OCP) crystal was chosen using low illumination intensity. A probe of 200 nm in diameter was used for 14 successive analysis of one minute each. The first point corresponds already to a value for the Ca/P atomic ratio of 1.45±0.05, too high with respect to 1.33 for OCP. Only a weak damage is visible after analysis at the centre of the probe image and the difference is too large to be accounted for an error in the standardless analysis of two K-lines of close elements. Then the Ca/P ratio becomes successively that one of tricalcium phosphate (TCP: 1.5),

[1] APFIM: Atom Probe Field Emission Microscopy, 3DAP: 3-dimensional atom probe

hydroxyapatite (HAP: 1.67) and even higher. The error bars correspond to a relative error of some ±5% with a 65% interval of confidence for the conditions used. Crystals in natural bone are typically 20-50nm wide and much thinner. Reducing the probe diameter to that level while keeping the same electron flux and analysis time would reduce the total count numbers, thus reduce the analysis accuracy beyond the limit where HAP, TCP and OCP can be distinguished from each others. Reducing the beam diameter to the same level while increasing the electron flux or the analysis time to keep the measured signal constant (i.e. the total electron dose constant) would induce during the first analysis already a composition change larger than the differences between these phases. Only EELS that brings a better efficiency in signal collection could allow analysing areas or particles of these materials on areas smaller than some 200nm with an acceptable accuracy after proper calibration of ionisation cross-sections for the actual experimental conditions. Nowadays the ability of the sample to withstand the electron probe is more often the ultimate limits to highly localized analysis rather than the sample holder drift.

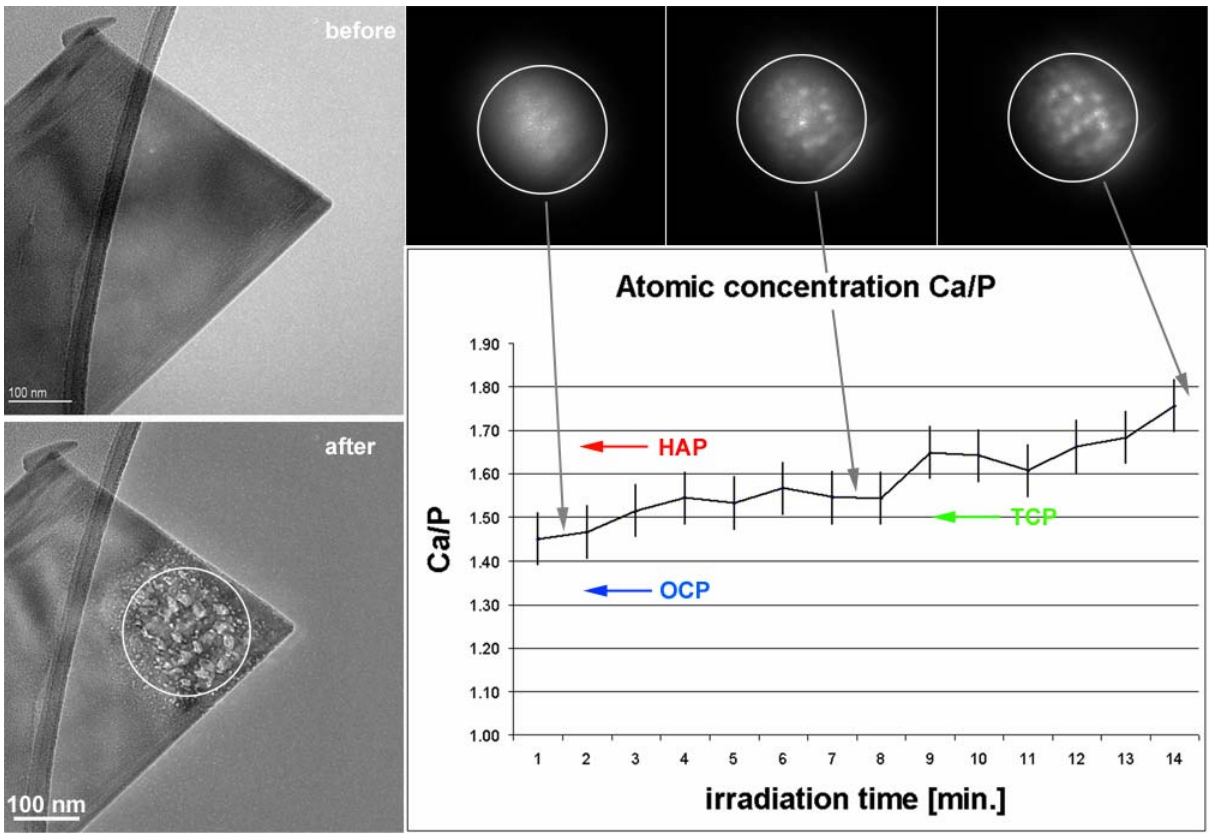


Fig. 1: EDS determination of the Ca/P ratio in an octacalcium phosphate synthetic crystal. This example shows that despite the care taken in setting up the analysis, significant loss of Ca occurred already before or during the first minute analysis. Then the apparent Ca/P ratio increases with irradiation and fits the TCP and HAP composition successively.

ii) Uncontrolled X-ray absorption may occur in the sample itself, particularly when it is not perfectly flat (bending of the thin foil, preferential etching during preparation, bars of the supporting grid...) or at the edge of the sample holder with detectors behaving a low take-off angle or even at the edge of the detector collimator when not aligned properly. Absorption is stronger for weak X-rays (unless an absorption edge is encountered) and this effect may be noticeable when two lines of the same element (K and L for instance) exhibit an abnormal ratio.

iii) Electron channelling has been considered as a method to gather information about site occupancy and is often referred as the ALCHEMI technique; see for instance Spence [5] and references herewith. But it is too often ignored that it is an important source of bias in apparent concentration for simple analysis and may change the apparent concentrations by several tens of per-cents or even more under strong diffraction conditions (fig. 2). As channelling affects the ionisation efficiency, it concerns both EDS and EELS analysis.

At the entrance face of the thin foil, the electron beam has a uniform density over the entire surface and ionisation occurs in proportion of the ionisation cross-section of each atom species and of its concentration. However during its travel through matter the electron waves are focused on some or all atom columns depending of the orientation and thickness of the foil (this constitutes the source of HRTEM images contrast) and the probability to ionise atoms on specific sites varies accordingly. When atomic species are not uniformly distributed on these sites, that is most often the case, some will be at total more efficiently ionised than others leading to a biased apparent concentration (fig. 2).

In phase analysis both diffraction on zone axis and EDS/EELS are often performed together, so care should be taken to tilt the sample out of the zone axis to the weakest diffraction conditions before performing the microanalysis. Acquiring concentration profiles at interfaces lying on low index crystallographic planes, as often encountered in semiconductors for instance, require a tricky balance between strong channelling when the interface is seen precisely edge-on giving best spatial resolution but also strong diffraction conditions and loss of spatial resolution on the projected interface when its plane is more or less tilted out of the illumination direction [6].

Channelling effects on microanalysis in the TEM may be reduced by using a large illumination aperture (condenser aperture) for microanalysis. It is not worthless to mention that in the SEM multiple scattering in bulk sample reduces electron channelling effects in EDS microanalysis to a negligible value most often.

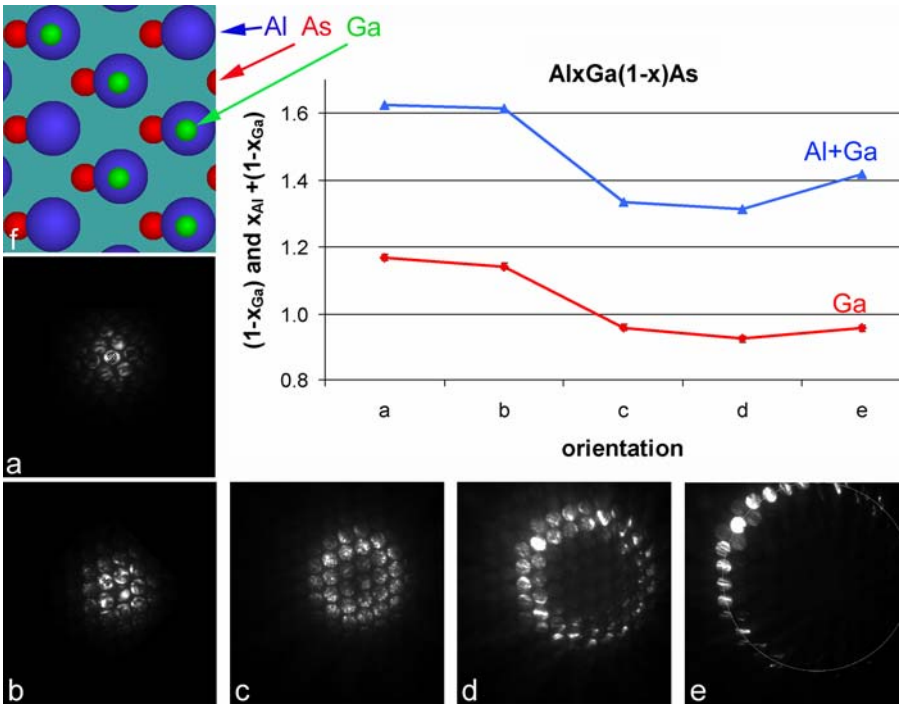


Fig. 2: Channelling effect in $Al_xGa_{1-x}As$. The projected structure (f) along [110] contains pure As atom columns (red) and mixed Al/Ga columns (green/blue). In this example, the electron wave was in average more focused on the Al/Ga atom columns than on the As ones. The stoichiometry is no longer satisfied by the apparent concentration: the compound looks like $Al_{xAl}Ga_{(1-xGa)}As$ where $x_{Al}$ and $x_{Ga}$ are no longer the same and the sum $x_{Al}+(1-x_{Ga})$ differs from unity by some 60%.

iv) Stray signals that the detector collimator cannot discriminate arise from the interaction of scattered electrons or X-rays with the sample or its surrounding (fig. 3a). Quite often, they constitute a large part in not the main part of the EDS spectrum in nano-scale analysis.

The "hole count" corresponds to the sample ionisation by the X-ray and the electron "showers" produced in the illumination part, mainly on the final condenser lens aperture and beyond. It is present even when the probe itself falls in a hole of the sample. This signal has long been recognized and is now reduced by the use of proper materials and shielding. Although still often invoked it is nowadays not the main source of inaccuracies and it can be removed more or less accurately by subtraction of a spectrum acquired slightly out of the sample edge.

More severe effect, the electrons forward and back- scattered out of the probe by the sample itself create an intense signal when hitting the bulk part of the sample itself or the components of the microscope (sample holder, anticontamination blades and objective pole pieces). In addition, some of these electrons are backscattered again to the sample. Removal of these contributions by the collimator of the EDS detector is by far imperfect. As the intensity of these effects depend of the scattering properties of the actual sample (composition, thickness, orientation, roughness and planarity...), they cannot be subtracted using some

reference spectra. In that respect the use of very small thin foils without large bulky parts, as produced by FIB cutting or extraction replica for instance, becomes a decisive advantage in EDS analysis when the feature of interest and its surroundings contain some elements in common that are searched for (coatings on substrate, precipitates in matrix, trace analysis in non-miscible phases...).

Figure 3c corresponds to an EDS analysis in the TEM of the matrix of WC-Co cermet coating deposited on steel (300 kV, 10 nm probe and the sample tilted 20° towards the EDS detector). Foreign elements are found and the relative concentrations between the metal elements reach some 2 at% Cr, 7 at% Fe and 5 at% Ni that is a stray signal coming from the steel substrate. This suggests that at least a part of the 30 at% W observed in the matrix together with the 24% Co should be attributed to the surrounding carbides rather to the matrix itself. The presence of 16 at% Mo corresponds to the washer used to hold the sample cross-section and the 16 at% Cu to the sample holder itself. On figure 3b, the EDS spectra were obtained in a SEM at 10mm working distance and 20 keV on a large area of the WC-Co coating. Only W, Co and a tiny C peaks are observed. Stray signals from the steel becomes negligible because of the stronger interaction of the probe in the underlying bulk material at the analysis position and of the better efficiency of the detector collimator with a longer space between the pole-piece and the sample.

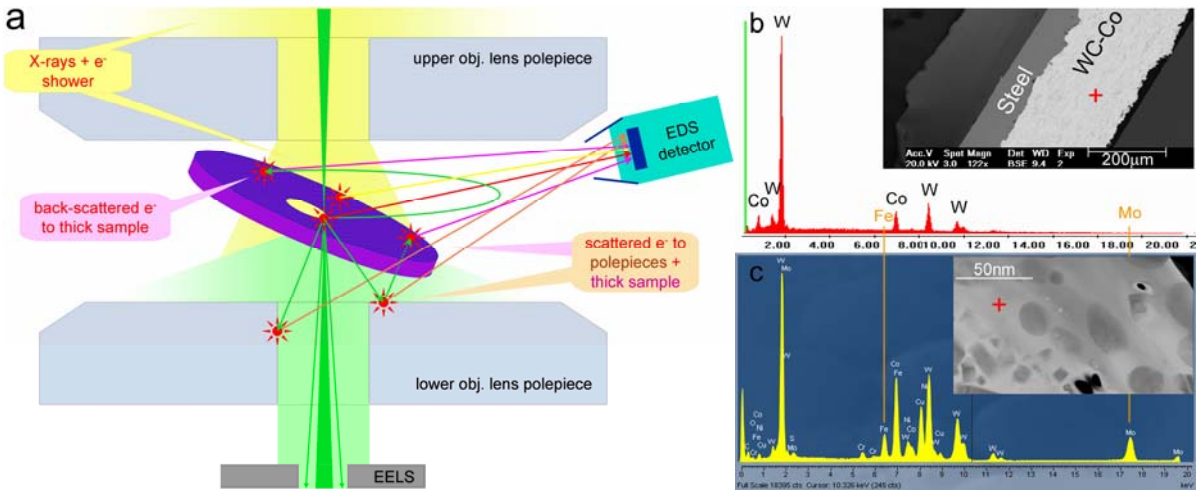


Fig. 3: a): stray X-ray photons are produced by the X-ray and electron showers falling from the condenser aperture on the sample, electrons scattered by the sample towards the pole pieces and backscattered electrons trapped in the magnetic field of the lens and hitting thick parts of the sample and sample holder. b) SEM-EDS spectra of a WC-Co cermet: stray signals are negligible. c) TEM-EDS point analysis of the matrix of a WC-Co cermet: Fe-Cr-Ni from the far steel substrate, Mo from sample support and Cu from sample holder are superimposed to the cermet matrix spectra and suggest that a large part of the W attributed to the matrix belongs in fact to carbides.

The accumulation of carbon under the probe (ashes of hydrocarbons brought by surface diffusion and destroyed by electron irradiation) takes the form of "contamination hills" with a high aspect ratio on both faces of the sample and constitutes another source of analysis delocalisation by beam broadening and scattering (fig 4). The sample preparation process, the way the thin foil is handled (keep bare hands off!) and kept (some polymer boxes left under sunshine on a desk may create awful hydrocarbon contamination!) are the most prominent hydrocarbon sources at contrary of the microscope vacuum itself. The old, but efficient, route of freezing the hydrocarbon mobility by cooling the sample at liquid nitrogen temperature is no longer practicable at high spatial resolution because of the prohibitive drift induced by thermal dilatation of the side-entry goniometre components or requires specially designed sample stages. But cleaning of the sample once mounted on the microscope sample holder in a low energy oxygen-rich plasma seems to have solved the problem as long as it does not remove carbon belonging to the sample itself (the carbon supporting film for particulate samples for instance when the cleaning process is applied too long).

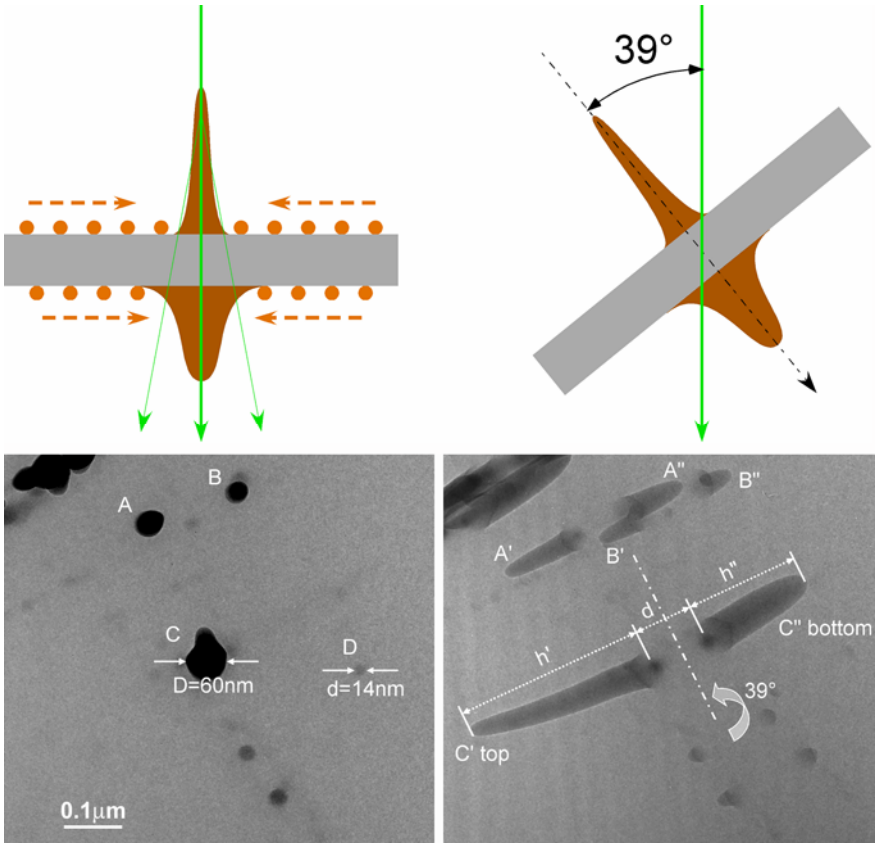


Fig. 4: Contamination spots on a GaAs thin foil under a probe 14 nm in diameter. Left: after a few seconds, the light contamination spot (D) has still nearly the diameter of the probe , after one minute (B) and some 200 seconds (C), the spots become darker and larger. Right: tilting the sample out by $\alpha$=39° the roots of the spots C' and C" are distant by d=0.10 $\mu$m that correspond to 160 nm foil thickness. The hill C' on the entrance face is thinner and longer (0.53$\mu$m) than on the exit face

C" because scattering broadens the beam on its path. The curvature of C' indicates a sample or probe drift during irradiation.

iv) Composition fluctuations within the analysed volume.

Assuming that the sample is a foil thin enough to prevent a significant probe broadening by electron scattering and that delocalisation of the interaction is negligible, the analysed volume is ideally a cylinder defined by the probe diameter and the sample thickness. Thus lateral resolution can reach nowadays the nanometre, even the atomic level when using ultrathin probes from modern microscopes with aberration corrected optics. However thin foils are several tens of nanometres thick at least and often composition is not uniform along the electron path (for instance for precipitates in a matrix or changes in surface composition induced by thinning artefacts) or nano-particles lie on a substrate. Thus, the analysis results reflect no longer the phases composition but some averaging between them and most often in an unknown proportion.

A similar averaging effect occurs when the sample or probe drifts. Keeping the probe on a nano-sized feature long enough for EDS signal collection remains still difficult with present sample stages and waiting for drift stabilisation at the level of the nm/minute constitutes the bottleneck in daily use.

EDS and EELS spectrometries are the most straightforward techniques to get chemical composition. However, when electrons interact with more than one phase the result of analysis is only an average composition. In several respect, EELS appears as a much more accurate technique than EDS and should be preferred. It is not sensitive to spurious signals from electrons scattered out of the observed feature and acquisition of the information is much a faster thus less sensitive to sample drift and contamination. However, EELS qualitative and quantitative analysis remains still more difficult than with EDS in most cases. Several spectra with different energy windows may be needed to cover all elements under investigation, fine tuning of the spectrometer and energy rescaling are still required quite often, choice of optimum parameters (ionisation edge, collection angle...) as well as less integrated software for spectra handling and quantitative interpretation require more operator skill than EDS nowadays.

**Electron Diffraction**

Crystallographic techniques based on electron elastic scattering are in numerous situations more selective tools for phase identification than spectrometries in the sense that a crystal lattice is a well defined property not at all or very weakly affected by the surroundings. Diffraction patterns from mixtures of crystalline phases superimpose but do not average the primary information that is distances and angles between spots constituting a periodic array. If necessary, dark field imaging can help to identify which reflection belongs to which phase. The main limitation comes from the existence of isomorphs compounds or at least with close lattices that cannot be distinguished due to the limited accuracy of experimental data. However, in such

cases, unambiguous solutions are often brought by a combination of elemental analysis by spectrometries to narrow the number of possible phases and diffraction.

The part of the sample contributing to the diffraction pattern may be chosen by limiting the area observed with an aperture. For technical reasons, it is done by inserting a "Selected Area Electron Diffraction" (SAED) aperture in the image plane of the objective lens rather than to the sample level itself. It can also be done by restricting the diameter of the illumination beam to the size of the feature of interest.

SAED is the most popular mode of getting diffraction patterns in a TEM. It has the advantage of giving sharp reflections as the illumination can be as parallel as the microscope design allows (be cautious with illumination aberrations and electron moving on helical paths in the objective lens [7]). Spherical aberration limits its ultimate spatial selectivity around 100nm by introducing a blur at the level of the SAED aperture that depends of the accelerating voltage, the diffraction angle and the spherical aberration coefficient $C_s$.

Defining the field by reducing the illuminated area was introduced long ago, but in old microscopes the poor optical performances of the condenser lenses did not allow to reach probes thinner than about a micrometre making the technique not really attractive. Nowadays modern probe forming optics and field emission electron sources lead to probes down to the nanometre range with still enough intensity to identify the area to analyse in a slightly defocused probe (NanoDiffraction nD) and then to record a pattern in a time short enough to keep the feature of interest under the focused probe despite of the sample drift.

However, first it should not be forgotten that in the absence of absorption the brightness of the gun $\beta = 4I/\pi^2 d^2 \alpha^2$ is kept constant all along the electron trajectories. Reducing the probe diameter d while keeping the same beam current I for constant visibility implies the angular aperture $\alpha$ to increase in a similar proportion at least (no aberrations were considered here for sake of simplicity). The situation becomes still worse when the coherence in illumination is present as for field emission guns [8]. In micro- or nano-diffraction, a condenser aperture as small as possible is used and the probe remains often slightly defocused to improve the beam parallelism at the price of an increased spot size. Convergent beam diffraction is not really different in the experimental set-up, but the condenser aperture is now larger to catch as much information as possible in the reciprocal space around the reflection and the probe is fully focused on the sample surface to increase the beam angular aperture on the one hand and to reduce the possible thickness fluctuations in the sample part under investigation on the other hand. The main limitation comes from the rapid contamination or the irradiation effects that occurs under the large electron beam density in the probe. Numerous samples are simply unable to withstand such an irradiation and decompose (see for instance fig. 1 on calcium phosphates), re-crystallise or even disappear by sublimation or electro-migration. Even if they are not so severe, dynamic effects under irradiation [9] may introduce more or less continuous changes in the lattice orientation in nanoparticles making the choice of a nanocrystal with suitable orientation uncertain if not undefined when such effects are fast compared to the exposure time.

An alternate method to nanodiffraction with very thin probes proceeds by recording crystallographic information in the direct space by high resolution transmission electron microscopy (HRTEM) and then getting access to the reciprocal space by Fourier transforming nanometre-sized selected areas of the HRTEM image into diffractograms. This approach is quite in favour although it is too often forgotten that diffractograms are not electron diffraction patterns, but only "pseudo-diffraction patterns" that mimic the geometry of the true diffraction patterns at best. The success of this approach comes from the relative ease for getting HRTEM images to who can access to a microscope with a limit of information around 0.15 nm, which is quite standard in materials science nowadays. Moreover HRTEM images of samples containing nano-crystals with random orientation always exhibit some of them close to a zone axis making the choice of the nano-area for "diffraction" more comfortable on micrographs than live in the microscope under the weak intensity of a defocused probe. The belief that irradiation damage is also lowered looks weak if not wrong as there is no improvement in signal collection efficiency, but maybe a better control of the total irradiation dose (searching for a suitable area and recording information). But this last point may dramatically change when more stable goniometre and illumination will allow to record a single STEM image at the nm-scale and then to move the probe on each particle or feature of interest and record its nanodiffraction pattern.

Fourier transform diffractograms of HRTEM images differ from the true diffraction patterns. First, the information about the phase of the diffracted beams is embedded in the interference pattern that is a HRTEM image, but is absent in classical diffraction patterns that map only the amplitude (as long as the reflection spots do not overlap). Second, the microscope transfer function adds some more phase changes and cut-off in the spatial frequencies transmission. Thus, the object is no longer a 3-D array of atoms but a 2-D lattice which contrast has no simple relationship with the former.

It is known that "image" of atom columns shifts from black to white spots (or even more complicated patterns) when the sample thickness changes. In rounded nanoparticles, the thickness is no longer constant over the whole object and the contrast of atom columns change from centre to the periphery. Moreover, the spacing between black or white spots (the "apparent" lattice) is larger close to the periphery than in the hart of the particle leading to bent "plane" images, suggesting a surface relaxation [10,11]. These effects are pure imaging artefacts and should not be confused with lattice change in nanoparticles with respect to the bulk material that results from physical reasons ("size effects") [12].

The diffractograms of such HRTEM images will thus behave maxima that do no longer represent the periodic atom lattice of the sample but the most prominent components of the Fourier space of a non periodic array. Some are close to the lattice periodicity, some suggests forbidden reflections that reappear from symmetry breakdown.

Multislice image simulations of a gold crystal bounded by a sphere of 14 fcc cells diameter have been calculated with JEMS [13] with a high sampling (2048x2048

pixels images, 0.001nm/pixel) and for a 300kV microscope (Cs=0.7mm, illumination half-convergence 1 mrad and defocus spread 4 nm). They show that the contrast of the atom columns along [001] is reversed from its centre to its periphery at the Scherzer defocus (45nm) and that the “lattice” is no longer strictly periodic (fig. 5a and c). The contrast reversal is no longer present at 95nm underfocus but on the outermost columns along {100} faces and only a small shift exists between white spots and projected potential maxima (fig 5b and d).

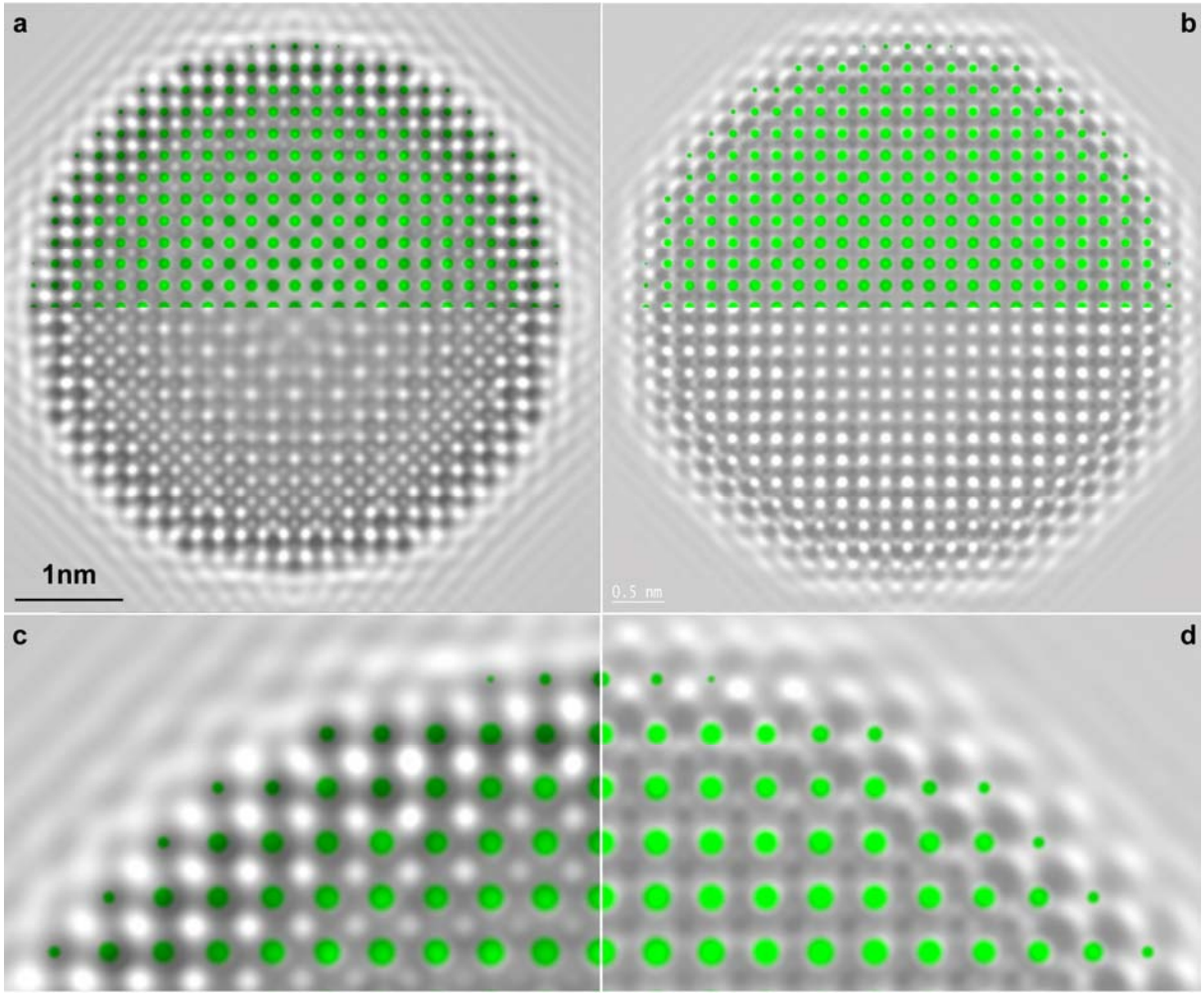


Fig. 5: Simulation of the HRTEM image of gold crystal 14 cells (5.7nm) in diameter viewed along [001] with the atom projected potential (green), a) Scherzer defocus (45nm) and b) 95nm underfocus for strong "lattice" contrast, c) and e) are details enlarged from a) and b) respectively to highlight the discrepancy between atoms position and "columns images".

"Lattice" spacings were measured on the equivalent of {200} and {220} spots on diffractograms (fig 6) of the simulated images with the DIFPACK module of DigitalMicrograph v 3.6.1 (Gatan). A refinement routine used in spot location finding allows a precision better than the image pixel size of 0.176 $nm^{-1}$/pixel [14]. Table 1 shows the difference between the HRTEM image "lattice" and the real lattice introduced in the model particle (bulk spacing a=0.4078 nm) for 45 nm (Scherzer), 65 nm, 87 nm (1st inverted transfer function maximum) and 95 nm underfocus

(quasi-periodic lattice). Results were also added for a 5.7 nm thick slab bounded by parallel faces (Au cell duplication 14 x 14 and (1+13) thickness iterations in JEMS) for sake of comparison with the case of a constant thickness sample. This latter shows that computing and sampling errors stay below 0.1%.

On experimental images, crystals exhibiting a 2-D lattice nearly never lie on a precise zone axis but close to it. This misorientation adds some more apparent lattice spacing and angle distortion. At total observed spacings may be increased up to 6 or even 8% as discussed for instance by Crozier [10] and Malm [15].

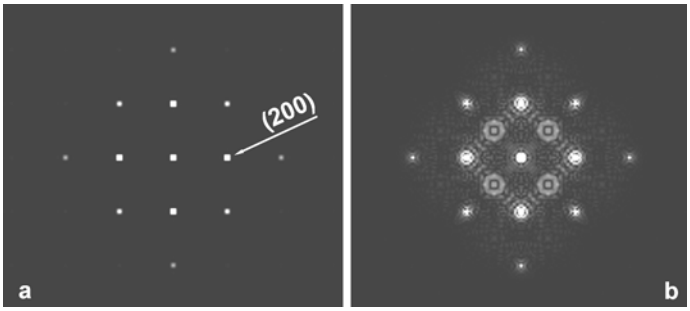


Fig. 6: Centre of diffractograms of the simulated image at Scherzer defocus: a) 14 x 14 cells thin foil, b) 5.7nm gold crystal with extra-spots from lattice distortions

**Table 1**: Difference between the HRTEM image "lattice" parameters measured on (200) and (220) diffractogram spots for a 5.7 nm thick slab and a 5.7 nm spherical nanocrystal at four different defocus, and the gold crystal parameter used to build the particle model.

| | difference to bulk lattice parameter | | | | |
|---|---|---|---|---|---|
| | slab | nano-crystal | | | |
| hkl \ defocus | 45nm | 45nm | 65nm | 87nm | 95nm |
| 200 | 0.0% | -3.0% | -2.8% | +2.5% | -0.3% |
| 220 | 0.0% | -0.3% | -1.3% | -2.8% | -0.4% |

In conclusion, HRTEM is an enticing route to gather crystallographic information from areas as small as a few nanometres. It requires an accurate comparison with simulated images that is no longer an issue in itself, but the uncertainty on the precise crystal orientation calls for automated routines that could calculate and fit simulated images not only for several objective lens defocus and crystal sizes, but also for a series of orientations around a zone axis. This stays still beyond the capabilities of present desktop computers. Using diffractograms to measure the average lattice looks much straightforward, but it should not be forgotten when interpreting these "pseudo"-diffraction patterns that the observed spacings may be shifted by several per cents out of the true crystal lattice. This explains why often comparing diffractograms of HRTEM images to crystal data with the standard 1-2% accuracy on spot position and camera length leads to "no solution".

**An example: Phase identification of an iron salt in Nafion**

Heterogeneous catalysts for photo-assisted degradation of organic pollutants under U.V.-visible light were prepared by impregnation with $Fe^{3+}$ ions in fluorinated polymer membranes (Nafion 117® Aldrich) [16].

A TEM investigation was undertaken to identify the morphology and nature of the iron compounds formed. Thin foils were cut by cryo-ultramicrotomy (Reichert Ultracut E/FC4D) with a Diatome 45° diamond knife at liquid nitrogen temperature. Observation was mainly performed with a Philips CM300UT/FEG operated at 300 kV ($C_s$ = 0.7mm, Scherzer resolution 0.17nm) and fitted with an Oxford Inca EDS and a Gatan GIF/EELS spectrometers. Images were recorded on a Gatan 797 slow scan CCD camera (1024 pixels x 1024 pixels 14 bit levels) under Digital Micrograph 3.6.1. The P. Stadelmann JEMS software [12] was used for HRTEM simulations and diffraction interpretation.

Bright and dark field images were first obtained under nearly low dose conditions with an illumination diameter as small as twice the area recorded by the CCD camera. This insures as much as possible that degradation of the polymer didn't induce a precipitation of the iron salt nor a particle growth under the beam and keeps fresh areas attainable by using the electronic image shift immediately before exposure. These pictures show the presence of 3-5nm rounded particles.

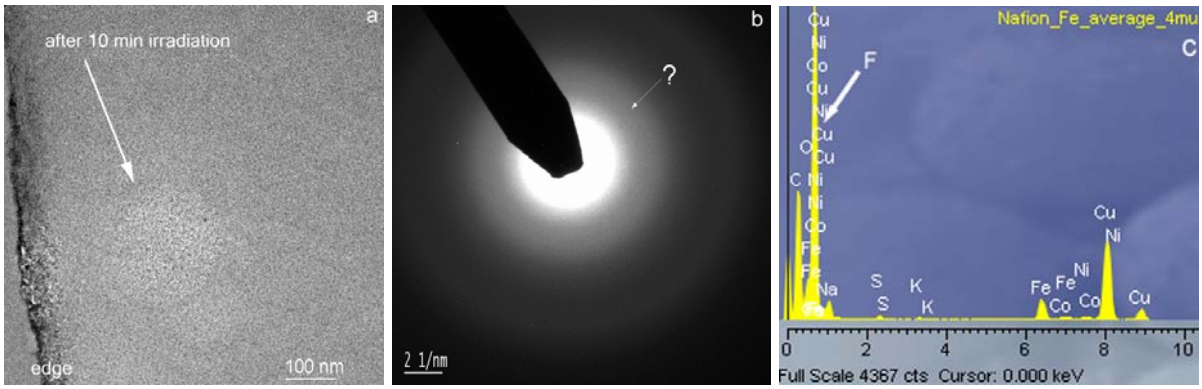


Figure 7: a) Bright field image of iron impregnated Nafion. Irradiation led to a slight mass loss of the sample and coarsening of the iron-rich particles. b) SAED diffraction pattern: only the broad rings of the amorphous matrix are clearly visible. c) EDS spectra show the presence of C, O, F, Fe (and Na, S and K traces) in the membrane. Ni, Co and part of Fe are a stray signals from the objective pole pieces and Cu from the supporting grid.

Further irradiation lets a lighter contrast in BF images showing that the polymer decomposes (fig. 7a). A slight change in the particle size is observed after a minute of irradiation, but remains low and it is assumed that only accretion of free standing molecules occurred without a chemical change.

Average EDS microanalysis with low probe intensity over areas some ten micrometres in diameter shows that the sample contain mainly C, O ,F, Fe and some traces of Na, K and S. Obviously hydrogen is also present. After discussion with the catalyst chemist, sulphur was considered to belong to the Nafion membrane itself

and was removed from the possible composition of particles. Then a list of 37 possible phases containing H, O, F and Fe or part of these elements was established using the PCPDF-win (Information Centre for Diffraction Data ) and ICSD (Inorganic Crystal Structure Database) databases and introduced in JEMS for diffraction spot pattern interpretation.

Even at the liquid nitrogen temperature, the Nafion membrane is still ductile and the thickness of the thinnest slices obtained by cryo-ultramicrotomy was still about 100nm, i.e. too large for analysis of the fine structure in EELS spectra. As the mass content of iron in the Nafion is about 1% and the particle size induces a strong reflection broadening, SAED diffraction patterns only exhibit broad rings as expected from the amorphous Nafion matrix and no or too weak rings from the particles to be useful for phase identification (fig. 7b). Nanodiffraction with a beam intensity still high enough to see the scene and to select the particles leads too rapidly to drill a hole in the polymer once re-focused on that particle. In addition, particles change their orientation rapidly during exposure. This was also observed on HRTEM images, but at least one particle with near zone axis orientation is found on each fourth CCD camera image recorded at a 510 kX direct magnification. To keep the irradiation damage as low as possible, HRTEM images are recorded "blind" within the first second after moving the beam with the electronic image shift on a fresh area and without any refocusing the objective lens.

First each part of the HRTEM images exhibiting a clear 2-D (zone axis) lattice was selected with a circular mask to remove the background from useless areas that would only contribute to enhance noise in diffractograms. The mask was bound with a Hanning filter to damp the edge effects during Fourier transform (fig 8).

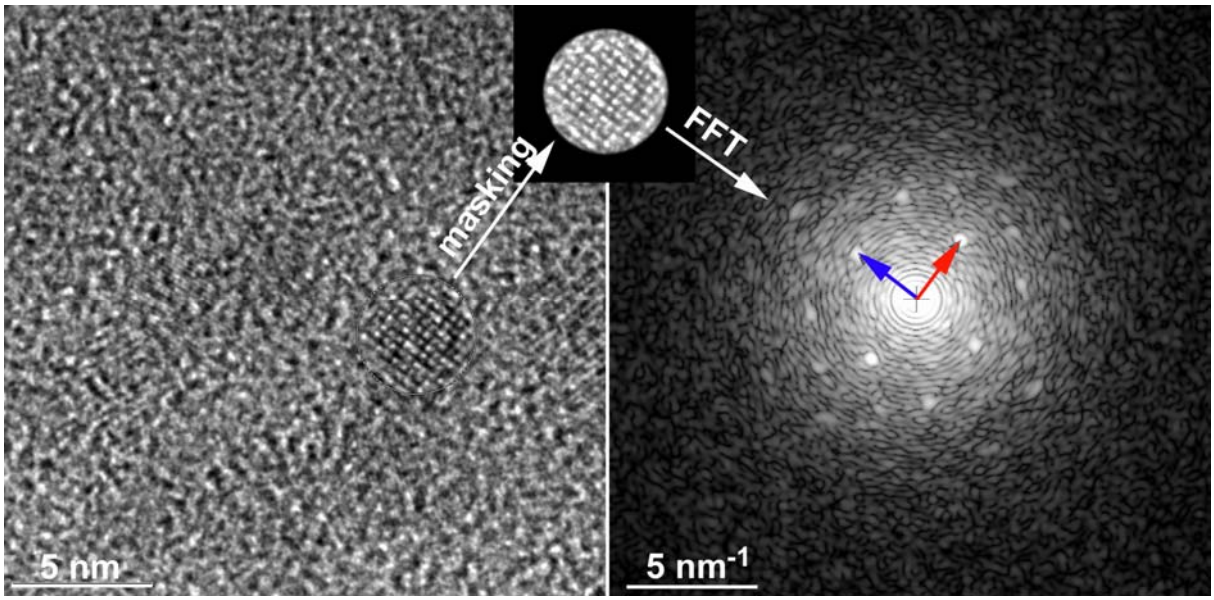


Figure 8: a): HRTEM image 1024x1024 pixels. b): Masking with a circular mask damped with a Hanning filter selects a single particle with 2-D lattice and removes the unnecessary amorphous parts that would contribute only to noise on the diffractogram. c): Diffractogram with the two vectors (red and blue) designing the spots that are used for indexation with JEMS.

Analysis of the diffractograms with an acceptable error of 3% on the spot position in JEMS and a range of possible camera length up to 2% out of the calibration led to about 10% successful indexations only and the remaining was left without solution. If in a few cases, the 2-D lattice was the result of two particles overlapping with 1-D lattice each, this situation was too seldom to account for the poor rating of indexation. It is quite unlikely that an unknown phase was present as no extreme pressure or temperature was used in the chemical reactions. Thus, the analysis was repeated with increased acceptable errors on spacing and to a less extent on angle also. However, it removed selectivity and led to an inextricable set of multiple solutions for each pattern.

Assuming that misorientation most often affect significantly only one of the two spacings on a zone axis, keeping the second one meaningful, and that sampling errors may average around the true spacing, all 1-D lattices on 50 micrographs were measured on diffractograms leading to some 700 interplanar spacings. In average, these values are equivalent to a list of plane spacings on a powder pattern and can be compared to that ones of the candidate phases having in mind that some bias may still be present on spacings in nanoparticles. To display the results each lattice measurement was plotted as a delta function versus the reciprocal of its spacing (blue bars on fig. 9) but the frequent overlaps make it hard to read. To get them on a form more readable, a gaussian of unit amplitude with a FWHM related to the confidence error was attached to each of these delta functions and all contributions were summed (black solid line on fig 9). Caution: this curve looks like the radial profile of a powder diffraction pattern, but it gives nothing else than the most often observed HRTEM "lattice" spacings! It is reasonable to assume that these maxima correspond or are close to crystal plane spacings in the sample. Thus, this curve allows a fast, visual comparison with planes in each candidate structure by highlighting those with planes in excess or missing. No single phase from the candidate list was able to explain all the spacings observed, but $FeF_2$ (ICSD-73729) fits the most prominent ones (light blue peaks on fig. 9a) and a second phase need to be considered at least. Chemistry strongly suggests that trivalent iron, probably an oxide or hydroxide, may be present and hematite $Fe_2O_3$ (ICSD-33643) explains the remaining maximum around 2.7 $nm^{-1}$. However, its $(1\bar{1}0)$ planes are not observed as often as it is expected and the (210) are not observed at all. One can argue that the operator may have introduced at start a bias by choosing a defocus giving the most often as possible "the best visibility of lattice images" that would correspond to the major phase $FeF_2$ crystals and that it could correspond to a low transmission of information for these two particular planes of $Fe_2O_3$. Such condition can be found around 53 nm underfocus, but then the (200) planes of $FeF_2$ should also be observed more rarely than it is the case. Eventually $FeF_3$ (ICSD-16671) appears a better candidate (with or without $Fe_2O_3$) to account for the spacings that do not correspond to $FeF_2$ (fig. 9b).

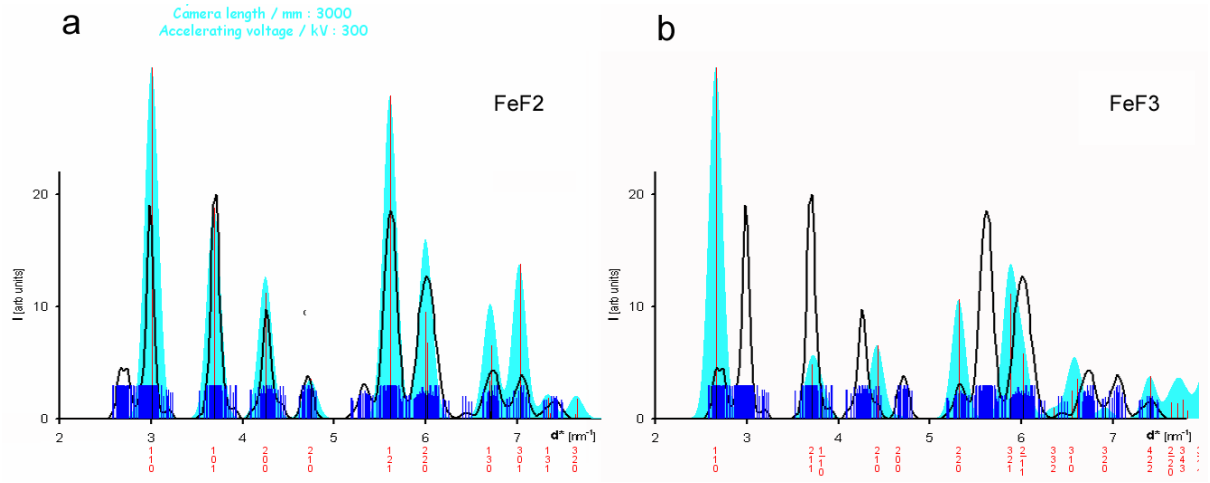


Figure 9: comparison of the most often measured atom plane spacings (in $nm^{-1}$) and their position for $FeF_2$ and $FeF_3$: the dark blue markers are the distances measured on diffractograms, the solid black curve their frequency obtained by attaching a gaussian of unit amplitude to each marker and summing all data and the light blue peaks figure the position of reflections on a true powder diffraction pattern.

The finding of two, possibly three phases in the Nafion membrane is a success for the technique of phase identification by analysis of HRTEM diffractograms in a complex situation in spite of the poor accuracy of plane spacings evaluation. The uncertainty that is left about the presence or the amount of hematite shows the importance to consider all possible phases and not to close the analysis as soon as one reasonable solution is found. $FeF_2$ and $FeF_3$ were not expected by chemists and thus not searched for by other techniques during the study. This keeps a slight doubt about a possible formation of these compounds under electron irradiation despite of the care taken to reduce the electron dose.

## Conclusion:

Both spectrometric and crystallographic techniques are required in the general case of phase identification even if from time to time an a priori knowledge allows to decide based on one technique only. Stray signals and composition averaging in the analysed volume by spectrometries lead only to an approximate composition knowledge of the phase under investigation that is often insufficient for conclusion. In many respects, EELS will be more performing than EDS (less stray signals, shorter analysis duration meaning less sample drift and irradiation damage) as soon as its use will become simpler thanks to better integration and computer assistance.

Diffraction is stricter than spectrometries as each phase keeps precisely its own lattice but is limited to crystalline materials and accuracy of experimental data may be insufficient to distinguish close lattices. Thus performing first a spectrometry approach to define a set of compounds to consider may be mandatory or at least may reduce the need for high accuracy diffraction information as well as the interpretation time.

Full matching of HRTEM images with models on simulated images is restricted to the cases where only a few phases are considered and the image contrast is sufficient. For nano-phases, the substrate superimposes a granular background that hides the fine details and only lattice spacings and angles can be measured on the image or its diffractogram. From the HRTEM image formation process, these data may differ from the crystal lattice itself by several per-cents in rounded or polyhedral particles. Thus, strict match of the observed HRTEM "lattice" with crystal lattice data should no longer be expected and identification can only be performed within a set of phases of reasonable size and not behaving too close lattices.

**Acknowledgements**

The author is very thankful to Prof. A. Czyrska-Filemonowicz for inviting him to give this lecture at the 1st Stanisław Gorczyca Summer School on Advanced Transmission Electron Microscopy and to the European Microscopy Society for its support. He is also deeply indebted to his colleagues Dr. E. I. Suvorova, Dr. K. Leifer and Prof. P. Stadelmann for introducing him in the biomaterials field, channelling modelling and large image simulation.

**Bibliography**

[1] P.E. Batson, *Near-edge conduction band electronic states in SiGe alloys*, J. Electron Microscs. **49** (2000) pp.267-273

[2] D. Blavette *et al*, *Three-Dimensional Atomic-Scale Imaging of Impurity Segregation to Line Defects*, Science **286** (1999) pp.2317-2319

[3] A. Cerezo et al., *Three-dimensional atomic scale analysis of nanostructured materials*, Micron **32** (2001) pp.731-739

[4] E. Suvorova and P.A. Buffat, *Electron diffraction from micro- and nanoparticles of hydroxyapatite*, J.Microsc. **196** (1999) pp.46-58

[5] J.C.H Spence, M. Kuwabara and Y. Kim, *Localization effects on quantification in axial and planar ALCHEMI*, Ultramicroscopy **26** (1988) pp103-112

[6] K. Leifer et al, *Theoretical and experimental limits of the analysis of III/Vsemiconductors using EELS*, Micron 31 (2000) pp.411–427

[7] K. K. Christenson and J. A. Eades, *Skew thoughts on parallelism*, Ultramicroscopy **26** (1988) pp.113-132

[8] C. Mory, M. Tencé and C. Colliex, *Theoretical study of the characteristics of the probe for a STEM with a field-emission gun*, J. Microsc. Spectrosc. El **10** (1985) pp.381-387

[9] P.A. Buffat, *Electron diffraction and HRTEM studies of multiply-twinned structures and dynamical events in metal nanoparticles: facts and artefacts*, Mat. Chem. Phys. **81** (2003) pp.368–375

[10] M. Flueli, Ecole Polytechnique Fédérale de Lausanne thesis n°796 1989; P.A. Buffat et al., *Crystallographic structure of small gold particles studied by high-resolution electron microscopy*, Faraday Discuss. **92** (1991) pp173-187

[11] P.A. Crozier *et al*., *Factors affecting the accuracy of lattice spacing determination by HREM in nanometre-sized Pt particles*, J. Electron Microscopy **48** (1999) pp.1015-1024

[12] C. Solliard and M. Flueli, *Surface stress and size effect on the lattice parameter in small particles of gold and platinum*, Surf. Sci. **156** (1985) pp.487-494

[13] P.A. Stadelmann, *Electron Microscopy Software Java Version*, http://cimewww.epfl.ch/people/stadelmann/jemsWebSite/jems.html

[14] W.J. de Ruijter *et al*., *Measurement of lattice-fringe vectors from digital HREM images: experimental precision*, Ultramicroscopy **57** (1995) pp.409-422

[15] J.O. Malm and M.A. O'Keefe, *Deceptive "lattice spacings" in high resolution micrographs of metal nanoparticles*, Ultramicroscopy **68** (1997) pp.13-23

[16] J. Kiwi et al., *Catalytic Fe3+ Clusters and Complexes in Nafion Active in Photo-Fenton Processes. High-Resolution Electron Microscopy and Femtosecond Studies*, Langmuir (2002) pp.9054-9066